Development 137, 2939-2949 (2010) doi:10.1242/dev.048843

The same enhancer regulates the earliest *Emx2* expression in caudal forebrain primordium, subsequent expression in dorsal telencephalon and later expression in the cortical ventricular zone

Yoko Suda*, Kenji Kokura*, Jun Kimura, Eriko Kajikawa, Fumitaka Inoue and Shinichi Aizawa†

SUMMARY

We have analyzed *Emx2* enhancers to determine how *Emx2* functions during forebrain development are regulated. The FB (forebrain) enhancer we identified immediately 3′ downstream of the last coding exon is well conserved among tetrapods and unexpectedly directed all the *Emx2* expression in forebrain: caudal forebrain primordium at E8.5, dorsal telencephalon at E9.5-E10.5 and the cortical ventricular zone after E12.5. Otx, Tcf, Smad and two unknown transcription factor binding sites were essential to all these activities. The mutant that lacked this enhancer demonstrated that *Emx2* expression under the enhancer is solely responsible for diencephalon development. However, in telencephalon, the FB enhancer did not have activities in cortical hem or Cajal-Retzius cells, nor was its activity in the cortex graded. *Emx2* expression was greatly reduced, but persisted in the telencephalon of the enhancer mutant, indicating that there exists another enhancer for *Emx2* expression unique to mammalian telencephalon.

KEY WORDS: *Emx2*, Otx, Tcf, Smad, Enhancer, Diencephalon, Telencephalon, Mouse

INTRODUCTION

In the mouse brain, *Emx2* is first expressed in caudal forebrain primordium at embryonic day (E) 8.5 (3- to 8-somite stage) and after E9.5 in dorsal telencephalon, forming a gradient along the anterior-posterior and dorsomedial-lateral axes, with the highest expression in the caudal-dorsomedial domain (Simeone et al., 1992; Gulisano et al., 1996; Mallamaci et al., 1998; Suda et al., 2001). At E12.5, the cells in prethalamus, thalamus and non-commissure region of the pretectum are descendants of the cells that once expressed *Emx2* (Kimura et al., 2005). However, after E9.5, *Emx2* expression does not occur in the majority of the diencephalon. After E12.5, during cortical lamination, *Emx2* is expressed in proliferating cells in the ventricular zone and Cajal-Retzius cells in the marginal zone; it is not expressed in differentiated neurons in cortical plate or the intermediate zone (Gulisano et al., 1996; Mallamaci et al., 1998; Shinozaki et al., 2002). *Emx2* has thus been presumed to play an essential role in each step and site of forebrain development; this has indeed been demonstrated in mouse mutants.

Emx2;Otx2 and *Emx2;Pax6* double mutants displayed *Emx2* functions in diencephalon development (Suda et al., 2001; Kimura et al., 2005). *Emx1;Emx2* double mutants indicated *Emx* functions in the development of medial pallium (Pellegrini et al., 1996; Yoshida et al., 1997; Shinozaki et al., 2004); they also showed their roles in cortical lamination (Shinozaki et al., 2002). It is interesting to know how these *Emx2* functions are differentially regulated. A previous study by Theil et al. (Theil et al., 2002) identified an *Emx2* enhancer immediately upstream of the *Emx2* translational start site that directs the *Emx2* expression in dorsal telencephalon but not in caudal forebrain primordium at the 3- to 6-somite stage. This enhancer was proposed to comprise two elements, 450 base pair (bp) DT1 and 180 bp DT2, 1.0 kb apart, both of which were essential and sufficient to direct the expression in dorsal telencephalon, but had no activity in caudal forebrain primordium at E8.5. However, we have realized that the promoter region adjacent to the *Emx2* translational start site does not harbor any enhancer activities. With an aim to correctly map the enhancer and to identify the caudal forebrain primordium enhancer, we have examined the enhancer activities of 28 non-coding domains that are conserved among mouse, human, chick and *Xenopus* at the mouse *Emx2* locus.

Here we report that DT2 exists immediately upstream of the *Emx2* translational start site, but DT1 exists immediately 3′ downstream of the last coding exon. Among mouse, chick and *Xenopus Emx2* loci, DT1 is conserved at a domain we named θ but DT2 is not. DT2 is unnecessary to the enhancer activity of the DT1-θ domain. In addition, the θ domain has the enhancer activity not only in dorsal telencephalon but also in caudal forebrain primordium at the 3- to 5-somite stage. After E11.5, it has the activity in the cortical ventricular zone but not in cortical hem or Cajal-Retzius cells in the marginal zone. The enhancer is regulated not only by Tcf and Smad, but also by Otx. Two other sites for unknown transcriptional factors, TGTTTTTTGCATGCT-TCATTTGCTT and GTGCAAATCAGTTTAAGCAATTATC, were also demonstrated to be essential for the enhancer activity. Of note is that not only the *Emx2* expression in dorsal telencephalon after E9.5, but also the expression in caudal forebrain primordium at the 3- to 5-somite stage and in the ventricular zone at E15.5 was regulated by all these factors. Mutant mice that lack this enhancer indicated that the enhancer is indeed essential to *Emx2* expression

Laboratory for Vertebrate Body Plan, Center for Developmental Biology, RIKEN Kobe, 2-2-3 Minatojima Minamimachi, Chuo-ku, Kobe 650-0047, Japan.

*These authors contributed equally to this work
†Author for correspondence (saizawa@cdb.riken.jp)

Accepted 21 June 2010

during forebrain development. However, the mutants also indicated the presence of another enhancer for the *Emx2* expression in telencephalon unique to mammals.

MATERIALS AND METHODS

Genome data

Comparison of mouse *Emx2* genomic sequences with other species was conducted with the Berkeley Genome Pipeline and Genomic VISTA (Couronne et al., 2003) programs. Additionally, sequence alignment was confirmed with the BLAST program (Mayor et al., 2000). Putative transcription binding sites were predicted with the TFSEARCH program (Heinemeyer et al., 1998). The source of finch data is Ensemble Genome Data Resources, Sanger Center Institute (http://www.ensembl.org/index.html).

Genomic DNAs and their modification

Each mouse *Emx2* genomic domain and *Xenopus Emx2* θ domain was obtained by PCR with primers located more than 100 bp apart from the 5′ and 3′ ends of the domains conserved between mouse and *Xenopus*, except for the (ζ–η–θ) domain. A 6.8 kb fragment containing mouse *Emx2* exon 1-3 (mEmx2GA2) was isolated from a BAC clone. The (ζ–η–θ) domain was obtained as a 4.9 kb fragment by *Nru*I and *Not*I digestion of the mEmx2GA2 plasmid. The mouse θ domain (~0.7 kb) was obtained by PCR with the following primers: 5′-TCTGAGAGATCTTCCACTCT-3′ and 5′-GTACCCACAATACAAACTCC-3′. The *Xenopus* θ domain was obtained as an 809 bp fragment from *Xenopus tropicalis* genome DNAs by PCR with the following primers: 5′-ACTCAACAAACCGATTGCGAATGC-3′ and 5′-ATCGTAATAATCTGGGGTTGAGTC-3′. The DNAs were provided by the National Bio-Resource Project (NBRP) of the MEXT, Japan. The PCR products were confirmed by sequencing. Tcf and Smad binding sites were transversely mutated and Otx binding sites (TAATCC) were mutated to GGCGCC, utilizing the PCR-based overlap extension method (Kucharczuk et al., 1999). Each 25 bp of the mouse N-fragment was replaced with a luciferase sequence (CTGGAGCCTGAGGAGTTCGCTGCCT) by the same method. All genomic DNA isolated or mutagenized by PCR was sequenced to verify the absence of spurious mutations.

Electrophoretic mobility shift assay

P19 cells expressing FLAG-HA-tagged Otx2 were established by transfecting the *Otx2* gene under the *E1a* promoter. The cells were neuralized by treating them with 1 nM retinoic acid from 24 hours after plating for a 48-hour period as previously described (Pachernik et al., 2005); the cells were further cultured for 48 hours in the absence of retinoic acid and nuclear extracts were prepared as previously described (Dignam et al., 1983). Under these conditions, the cells expressed early neuroectoderm marker *Sox1*, rostral brain markers *Otx1* and *Otx2*, forebrain markers *Emx2* and *Pax6*, and midbrain marker *Dmbx1*, but not hindbrain marker *Gbx2*, mesoderm marker *Bra* nor endoderm marker *Gata4*. Otx2 protein was isolated with FLAG-M2 beads (Sigma) as per manufacturer's instructions. The electrophoretic mobility shift assay was conducted as previously described (Takasaki et al., 2007).

Chromatin immunoprecipitation (ChIP) assay

The assay with the neuralized P19 cells was conducted as previously described (Agata et al., 2001). Otx2 antibodies were purchased from Chemicon (#1 in Fig. 6C) and R & D (#2 in Fig. 6B,C). The assay with E11.5 telencephalon was performed as previously described (Visel et al., 2009). Antibodies used were rabbit anti-Otx2 (ab21990, Abcam), rabbit anti-Tcf1 (C63D9, Cell Signaling), rabbit anti-Tcf4 (C48H11, Cell Signaling), rabbit anti-Smad1/5/8 (N-18, Santa Cruz Biotechnology) and rabbit control IgG (ab46540, Abcam) coupled to Dynabeads Protein G (Invitrogen). Primers for the PCR were p1 (5′-ACCAGGAATATGAAGGGAAAAGAGG-3′) and p2 (3′-GCATTGTAACTTGGCCTTATCACAG-5′), of which locations are indicated in Fig. 4B.

Mutant mice and animal housing

The isolation of the recombinant clones and production of the FB enhancer mutant mice (Accession No. CDB0073K) were performed as previously described (http://www.cdb.riken.go.jp/arg/download_file/vector_09.pdf). The primers used to identify the wild-type allele were p1 (5′-ATCAGTTTAAGCAATTATCATACCAG-3′) in the θ domain and p2 (5′-TGTAAGGAGACTATACTCTACTCTAT-3′) in its 3′ downstream domain (Fig. 8A); those used to identify the FB *neo* allele were p3 (5′-GTACTCGGATGGAAGCCGGTCTTGTC-3′) in the *neo* cassette and p2; those used to identify the ΔFB allele were p4 (5′-TCAATATGCCCTCAGAGTAGTTGTCT-3′) in front of the insertion site of the *neo* cassette and p2 (Fig. 8A). *Otx2*-null (Accession No. CDB0010K), *Emx1*-null (Accession No. CDB0021K) and *Emx2*-null (Accession No. CDB0018K) mutants and *Cre* knock-in mutant mice at the *Emx2* locus (Accession No. CDB0020K) were established previously and genotyped as described (http://www.cdb.riken.jp/arg/mutant%20mice%20list.html) (Matsuo et al., 1995; Yoshida et al., 1997; Kimura et al., 2005). ROSA26R mice were obtained from Jackson Laboratory (http://jaxmice.jax.org/strain/003474.html). Mice were housed in environmentally controlled rooms under the RIKEN Center for Developmental Biology (CDB) guidelines for animal and recombinant DNA experiments.

RT-PCR analysis

RNA isolation and semi-quantitative reverse transcription (RT) PCR were performed according to Kimura et al. (Kimura et al., 2001). Primer sets used were as follows: *Emx2*, 5′-CCGAGAGTTTCCTTTTGCACAACGC-3′ and 5′-GCCTGCTTGGTAGCAATTCTCCACC-3′; *HPRT*, 5′-GAAATGTCAGTTGCTGCGTC-3′ and 5′-GCCAACACTGCTGAAACATG-3′. Quantitative RT-PCR was carried out as previously described (Shibata et al., 2008). For all primer sets tested, correlation (R2) was higher than 0.98 and the slope was –3.1 to –3.6 in each standard curve. Primers to detect the expression of each gene were designed in a single exon encoding a 3′UTR: forward, 5′-CTGCACACACATCCACCGAG-3′, and reverse, 5′-GCGTCACTGCTCTGATTCCC-3′ for *Emx2*; forward, 5′-GTGATGTGAAGTTCCCCATAAGG-3′, and reverse, 5′-CTACTGAACTGCTGGTGGGTCA-3′ for *Tbp* (Svingen et al., 2009).

RESULTS

Emx2 enhancer that drives expression in forebrain

As true of mouse *Emx2*, chick and *Xenopus Emx2* genes are expressed in caudal forebrain primordium at neural plate stage, in dorsal telencephalon after neural tube closure and in ventricular zone of the developing cortex (Bell et al., 2001; Pannese et al., 1998). Therefore, we rationalized that the enhancers directing these expressions are conserved among tetrapods. We thus compared 556-kb non-coding genomic sequences between the genes adjacent to *Emx2* at the 5′ and 3′ ends (PDZK8 and Rab11FIP2) among mouse, human, chick and *Xenopus* (Fig. 1A). We chose 5 (α–ε) and 23 (ζ-ω5) domains at the 5′ and 3′ ends of the translational start site, respectively, as the domains conserved among tetrapods. The DT1 domain from Theil et al. (Theil et al., 2002) corresponds to the θ domain, whereas the DT2 domain is not conserved, being located between the γ and δ domains (Fig. 1B). A 2.1 kb region proximal to the translational start site (Fig. 1B) that covers the δ and ε domains did not express any apparent β-gal expression in E8.0-E15.5 transgenic embryos when fused with a *lacZ* reporter gene (*2.1-lacZ*). This 2.1 kb fragment was then used as the promoter in the enhancer assay; each domain was combined with *2.1-lacZ* and the enhancer activity was examined by generating transgenic embryos (Fig. 1C). It was only the (ζ–η–θ) domain that exhibited enhancer activities in anterior neuroectoderm and forebrain during E8.0-E15.5; this domain exhibited early activity in caudal forebrain primordium at the 3- to 6-somite stage.

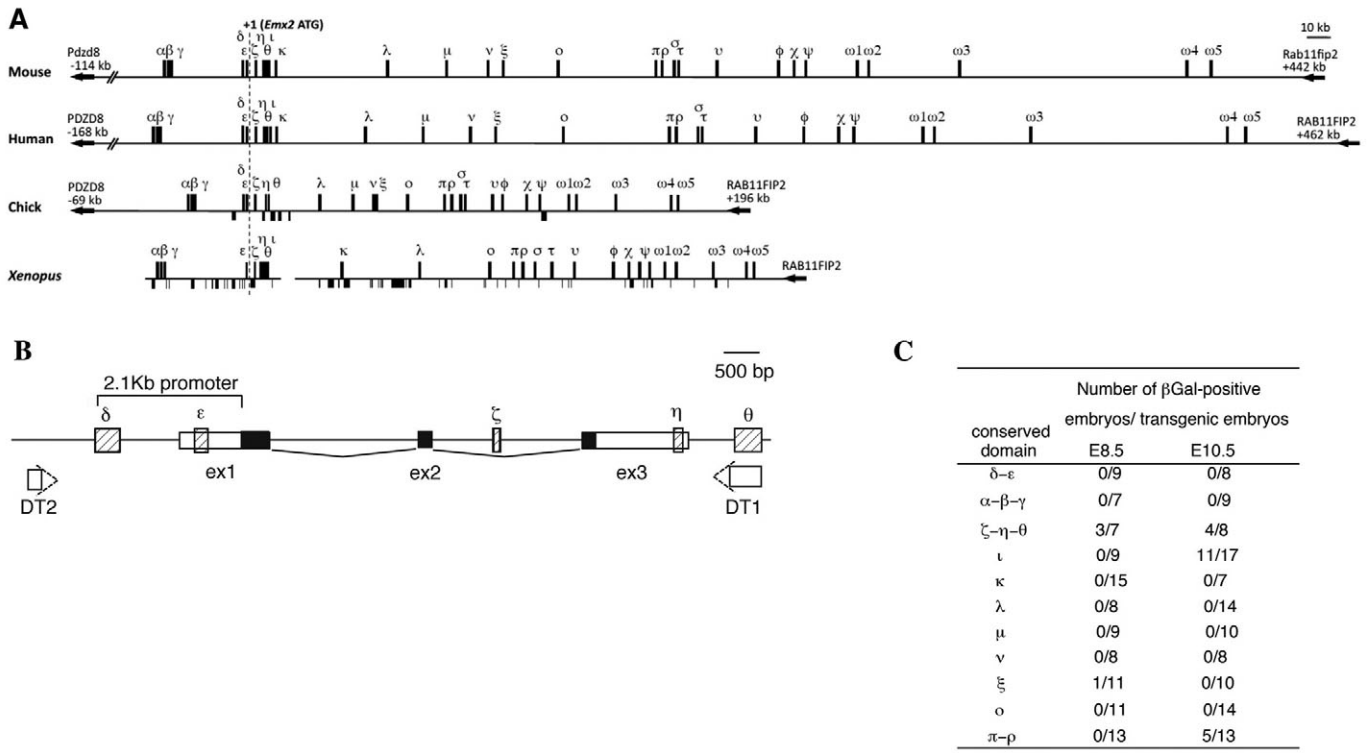

C

conserved domain	Number of βGal-positive embryos/ transgenic embryos E8.5	E10.5
δ–ε	0/9	0/8
α–β–γ	0/7	0/9
ζ–η–θ	3/7	4/8
ι	0/9	11/17
κ	0/15	0/7
λ	0/8	0/14
μ	0/9	0/10
ν	0/8	0/8
ξ	1/11	0/10
ο	0/11	0/14
π–ρ	0/13	5/13

Fig. 1. Enhancer activities of 28 domains conserved among tetrapod *Emx2* gene loci. (**A**) The location of the 28 domains in mouse, human, chick and *Xenopus Emx2* loci. Arrows at both ends indicate the adjacent genes, Pdzd8 and Rab11fip2 at 5′ and 3′ ends of the *Emx2* gene, respectively. In chick and *Xenopus*, the lower bars indicate sequences not determined. Domains ι and κ are not found in the chick genome, but there are undetermined sequences in the genome and the domains are well conserved in *Xenopus* and finch. A sequence gap exists at the proximal 3′ end of the *Xenopus* genome and δ, μ, ν and ξ domains are not identified in the *Xenopus* genome; however, they are well conserved in mouse, human, chick and finch genomes. The other 22 domains are conserved in exactly the same genomic arrangement among the tetrapod *Emx2* gene loci. (**B**) Detailed map of δ-θ domains and *Emx2* exons. White boxes show untranslated exons, black boxes show coding exons and hatched boxes show δ-θ domains. Locations of DT1 and DT2 from Theil et al. (Theil et al., 2002) and the 2.1 kb region used as the promoter in this study are indicated. (**C**) Transgenic analysis of enhancer activities at E8.5 and E10.5. *Emx2* is expressed in intermediate mesoderm that generates kidney and urogenital organs (Miyamoto et al., 1997). One among 11 transgenic embryos with the ξ domain exhibited this activity at E8.5, but none among 10 transgenic embryos had any activity at E10.5; more detailed analysis is required to determine the enhancer activity of the ξ domain. All the β-gal expressions observed in only one transgenic embryo with other domains were not at endogenous sites; they were considered ectopic by the effects of accidental integration sites of the transgenes and not counted as positive. At E10.5, *Emx2* is expressed in the root of trigeminal nerve (arrow in Fig. 2X), and five out of thirteen transgenic embryos with the (π–ρ) domain exhibited this activity (Fig. 2A). *Emx2* is also expressed in the mammillary region and non-commissure region of the pretectum (Kimura et al., 2005), and the ι domain had activities at these sites (Fig. 2B). We were especially interested in identifying the enhancer for the expression in caudal forebrain primordium, and the enhancer activities of far-3′ domains σ–ω5 were examined only at E8.5, none of them showing activities. The number of transgenic embryos generated and examined was: σ /τ, 8; υ, 9; φ, 9; χ, 10; ψ, 6; ω1, 6; ω2, 11; ω3, 6; ω4, 8; ω5, 6.

We then generated permanent transgenic lines that harbored (ζ–η–θ)-*2.1-lacZ* to compare temporal changes of the activities with the endogenous *Emx2* expression in detail (Fig. 2). The β-gal expression was first observed at the 3- to 6-somite stage in caudal forebrain primordium, as was endogenous *Emx2* expression (Fig. 2C,G). At E9.5, endogenous *Emx2* expression was found in telencephalon but not in diencephalic region (Fig. 2D,E). The β-gal expression, however, remained in the diencephalic region and was rarely found in the telencephalic region (Fig. 2H). At E10.5, β-gal expression was still retained in the diencephalon, but also occurred in a dorsocaudal part of the telencephalon (Fig. 2I,J); β-gal expression covered the entire diencephalon except for the commissure region of pretectum. At E11.5, the expression faded in the diencephalon and covered the entire dorsal telencephalon (Fig. 2K,L). Therefore, the enhancer activity of the (ζ–η–θ) domain shifted from the diencephalic region to the telencephalic region, as endogenous *Emx2* expression does, but the shift was delayed. Moreover, endogenous *Emx2* expression includes the cortical hem, although not the choroid plexus or choroidal roof, and is graded high dorsomedially in the cortex (Fig. 2F,M,M′,O). The activity of the (ζ–η–θ) domain did not include the cortical hem and was not graded in the cortex (Fig. 2L,N,N′,P). The endogenous *Emx2* expression was weakly found in the ventricular zone of lateral ganglionic eminences and a part of medial ganglionic eminences (Fig. 2M). The (ζ–η–θ) domain exhibited significant activities not only in the ventricular zone but also in the differentiating field of lateral ganglionic eminences; it had no activity in medial ganglionic eminences (Fig. 2N). In E15.5 cortex, endogenous *Emx2* expression is found in the ventricular zone and in Cajal-Retzius cells in the marginal zone, but not in the cortical plate or intermediate zone (Fig. 2Q,Q′) (Shinozaki et al., 2002). The majority of Cajal-Retzius cells originate from the *Emx2*-positive cortical hem (Takiguchi-Hayashi et al., 2004; Yoshida et al., 2006). The (ζ–η–θ) domain was active in the ventricular zone, but it had

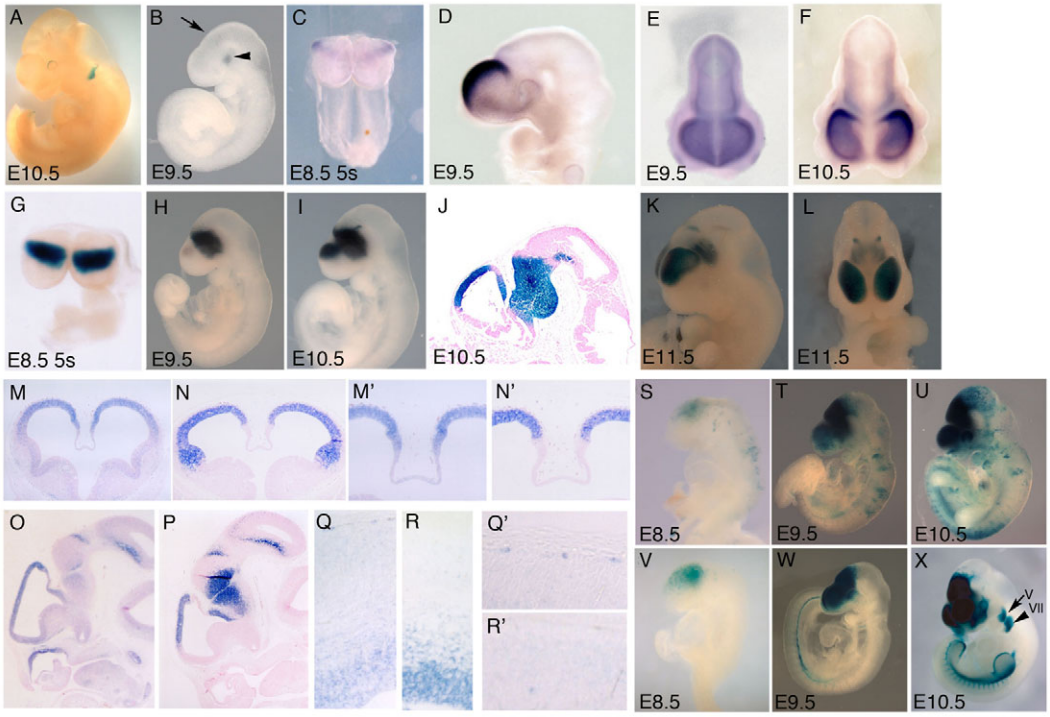

Fig. 2. Activities of enhancer-active domains. (**A**) β-gal expression in the root of trigeminal nerve by the (π–ρ) domain. (**B**) β-gal expression in the mammillary region (arrowhead) and non-commissure region of pretectum (arrow) by the ι domain. (**C-F**) Endogenous *Emx2* expression at stages indicated by wholemount RNA in situ hybridization. (**G-L**) β-gal expression directed by the (ζ–η–θ) domain at the stages indicated. J shows the expression in a parasagittal section. (**M-R′**) Endogenous *Emx2* RNA expression (M,M′,O,Q,Q′) and *lacZ* RNA expression (N,N′,P,R,R′) directed by the (ζ–η–θ) domain at E11.5 (M-P) and E15.5 (Q-R′) in coronal sections at a telencephalic level (M,N), in dorsomedial telencephalon (M′,N′), in parasagittal sections (O,P), in cortices (Q,R) and in the marginal zone (Q′,R′). (**S-X**) β-gal expression in ROSA26R embryos at indicated stages; the embryos were obtained by injecting the *Cre* gene under the (ζ–η–θ) domain (*A-Cre*; Fig. 3A) into ROSA26R zygotes (S-U) or by crosses of ROSA26R females with *Cre* knock-in males into the *Emx2* locus (V-X). The arrow in X indicates the expression in the root of trigeminal nerve and the arrowhead indicates the root of the facial nerve. A,B,D,H,I,K,S-X, lateral views; C,G, frontal views; E,F,L, dorsal views. Anterior is to the left in A,B,D,H-K,O,P,S-X.

no activity in the marginal zone (Fig. 2R,R′), coincident with the lack of the activity in the cortical hem (Fig. 2N,N′). These differences in the enhancer activities of the (ζ–η–θ) domain from the endogenous *Emx2* expression were commonly observed in three transgenic lines independently established. β-gal protein is relatively stable, and differences might exist between *lacZ* mRNA expression and β-gal protein expression. However, being directed by the (ζ–η–θ) domain, the expression pattern of the *lacZ* mRNA was almost the same as that of the β-gal expression.

At E11.5, *Emx2* is also expressed in part of the pretectum and tegmentum, and weakly in the thalamus, prethalamus and thalamic eminence (Fig. 2O). The (ζ–η–θ) domain had significant activities at these sites (Fig. 2P). Endogenously, *Emx2* is also expressed in the urogenital ridge (data not shown) and nasal epithelia (Fig. 2O). The (ζ–η–θ) domain did not have activities at these sites (Fig. 2P; data not shown).

The enhancer activities of the (ζ–η–θ) domain were also determined by injecting the (ζ–η–θ)-*2.1-Cre* transgene, in which the domain was combined with the 2.1 kb promoter and *Cre* gene (*2.1-Cre*), into zygotes from ICR females mated with homozygous ROSA26R mice; the β-gal expression in the embryos developed from the zygotes represents all the cells in which the (ζ–η–θ) domain was at one time active. The expression was found in caudal forebrain primordium at E8.5 and in telencephalon and diencephalon at E10.5 (Fig. 2S-U). This is as observed in ROSA26R embryos obtained by cross with $Emx2^{+/Cre}$ mice in which the *Cre* recombinase gene was knocked-in into the *Emx2* gene locus to be expressed in place of *Emx2* (Fig. 2V-X). Of note is that the (ζ–η–θ) domain exhibited activity in telencephalon at E9.5 in this assay (Fig. 2T).

Core domain

In dissecting the enhancer activities of a 4.9 kb *A* fragment that covers the (ζ–η–θ) region, we took advantage of the Cre-ROSA26R system by which enhancer activities both at earlier stages in caudal forebrain primordium and at subsequent stages in telencephalon can be determined by a single assay at E9.5. The *C* (3.1 kb), *F* (1.8 kb), *G* (1.0 kb) and *Q* (0.7 kb) fragments retained enhancer activities the same as the 4.9 kb *A* fragment; the activity was finally confined to the 400 bp *Bgl*I-*Hin*dIII fragment (*N*) (Fig. 3A,Ba-d). Further dissection of the *N* fragment into three fragments (*R*, *S* and *T* in Fig. 3A) abolished activity both in caudal forebrain primordium and telencephalon; the middle *T* fragment exhibited aberrant activity (Fig. 3Be) and the 5′ *R* or 3′ *S* fragment exhibited no activity (Fig. 3A). The activity of the *N* fragment was also examined by combining it with *2.1-lacZ* (Fig. 3C). It exhibited the same activity as the (ζ–η–θ) domain (Fig. 2). However, the shift of its activity from diencephalon to telencephalon took place earlier than the (ζ–η–θ) domain, although still later than endogenous *Emx2* expression. The *N* fragment coincides with the DT1 element from Theil et al. (Theil et al., 2002) and the θ domain conserved among tetrapod *Emx2* loci (Fig. 1A,B); we refer here to the enhancer existing in the *N* fragment or θ domain as the FB (forebrain) enhancer.

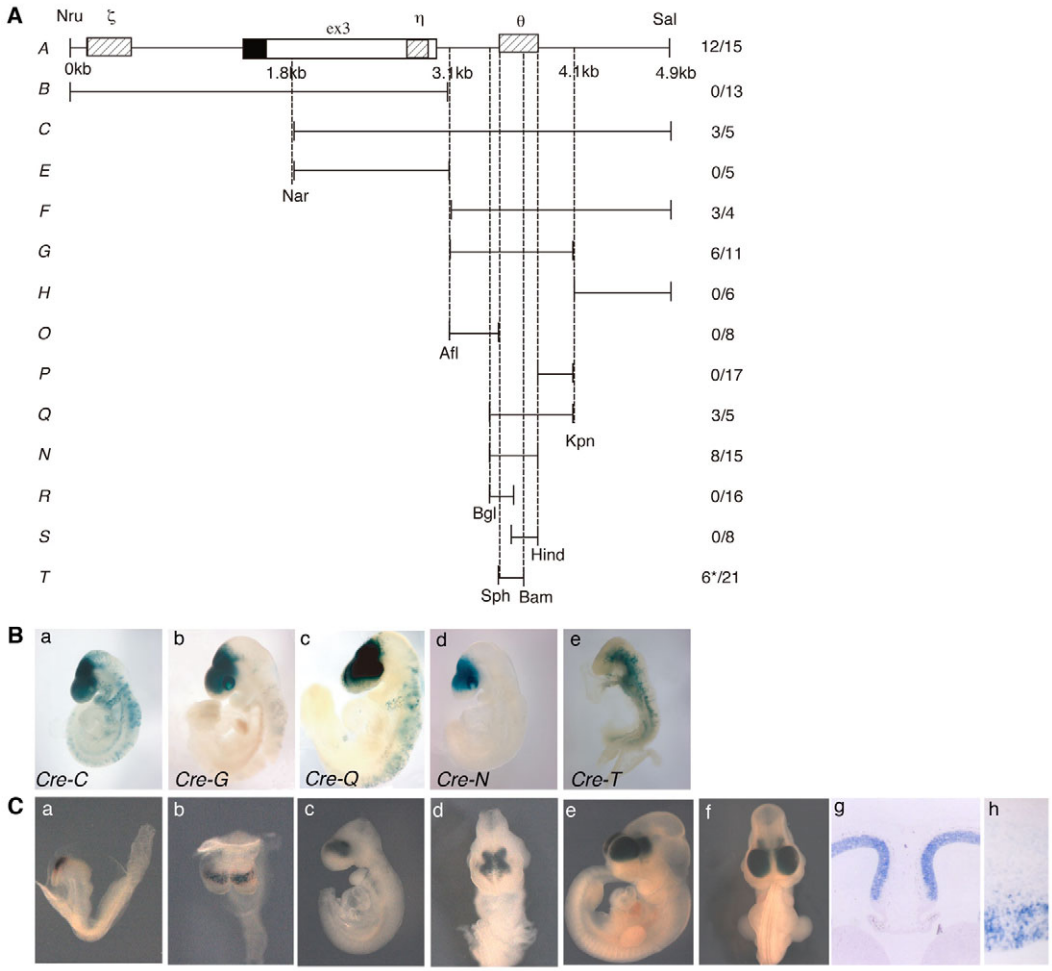

Fig. 3. Deletion analysis of the enhancer activity of the (ζ–η–θ) domain. (**A**) Schematic representation of deletion constructs. The number of β-gal-positive embryos among total E9.5 transgenic embryos generated is given at the right. The asterisk indicates aberrant activities shown in Be. (**Ba-e**) β-gal expression of E9.5 ROSAR26 embryos injected with the *Cre* gene, directed by each fragment indicated. Ectopic activity was found in eyes with the *G*, *Q* and *N* fragments. All are wholemount lateral views with anterior to the left. (**Ca-h**) β-gal expression in a transgenic mouse line harboring the *lacZ* gene directed by the *N* fragment at E8.5 (a,b), E9.5 (c,d), E10.5 (e,f), E12.5 (g) and E15.5 (h). a,c,e, lateral views with the anterior to the left; b,d,f, frontal views; g,h, coronal sections at a telencephalic level (g) and the cortex (h).

Significance of Otx, Tcf and Smad binding sites

The nucleotide sequence of the θ domain was deeply conserved not only among amniotes but also in *Xenopus* (Fig. 4A,B). Smad and Tcf binding sites are present in the mouse θ domain as reported by Theil et al. (Theil et al., 2002), and they are conserved among tetrapod *Emx2* θ domains. In addition, two potential Otx binding sites exist in *Emx2* θ domains of these animals (Fig. 4B). To examine whether these sites are indeed essential to the FB enhancer activities in caudal forebrain primordium and telencephalon, the enhancer activities of the *N* fragments in which mutation or deletion was introduced into these sites were examined by the Cre-ROSA26R system (Fig. 5). The transverse mutation of the Smad binding site reduced β-gal expression at E9.5 (Fig. 5Bb), and β-gal expression was residual when the Tcf binding site was transversely mutated (Fig. 5Bc). Mutation in both Tcf and Smad sites abolished β-gal expression completely (Fig. 5Bd). In addition, both deletion and transverse mutation of the two Otx binding sites abolished the activities of the *N* fragment in both diencephalon and telencephalon (Fig. 5Be,f). Tcf, Smad and Otx binding sites were also essential to the activity in the E15 cortical ventricular zone (Fig. 5Bg-i).

Otx2 protein binding to Otx sites

Smad and Tcf were reported to bind to the Smad and Tcf binding sites, respectively, by Theil et al. (Theil et al., 2002). Electrophoretic mobility shift analysis was conducted to demonstrate that Otx protein also binds to the potential binding sites in the 0.4 kb FB enhancer. The Otx2 protein, isolated from neuralized P19 cells expressing *FLAG-HA*-tagged *Otx2* under the *EF1a* promoter (see Materials and methods), yielded a uniquely shifted band (Fig. 6B, lanes 1 and 2). This band was almost lost in competition with a wild-type competitor (Fig. 6A, WT; Fig. 6B, lanes 3 and 4) or mutant competitors in which only one of the two Otx sites was mutated (Fig. 6A, 1M and 2M; Fig. 6B, lanes 5-8). However, the shifted band was not lost in competition with a mutant competitor in which both Otx sites were mutated (Fig. 6A, 1-2M; Fig. 6B, lanes 9 and 10). Furthermore, anti-Otx2 antibody super-shifted the band (compare lanes 11 and 12 in Fig. 6B), suggesting that the complex represented by the shifted band indeed contains Otx2 protein.

We next performed a chromatin immunoprecipitation (ChIP) assay to confirm that endogenous Otx binds to these Otx sites. The ChIP assay with the neuralized P19 cells was conducted with two

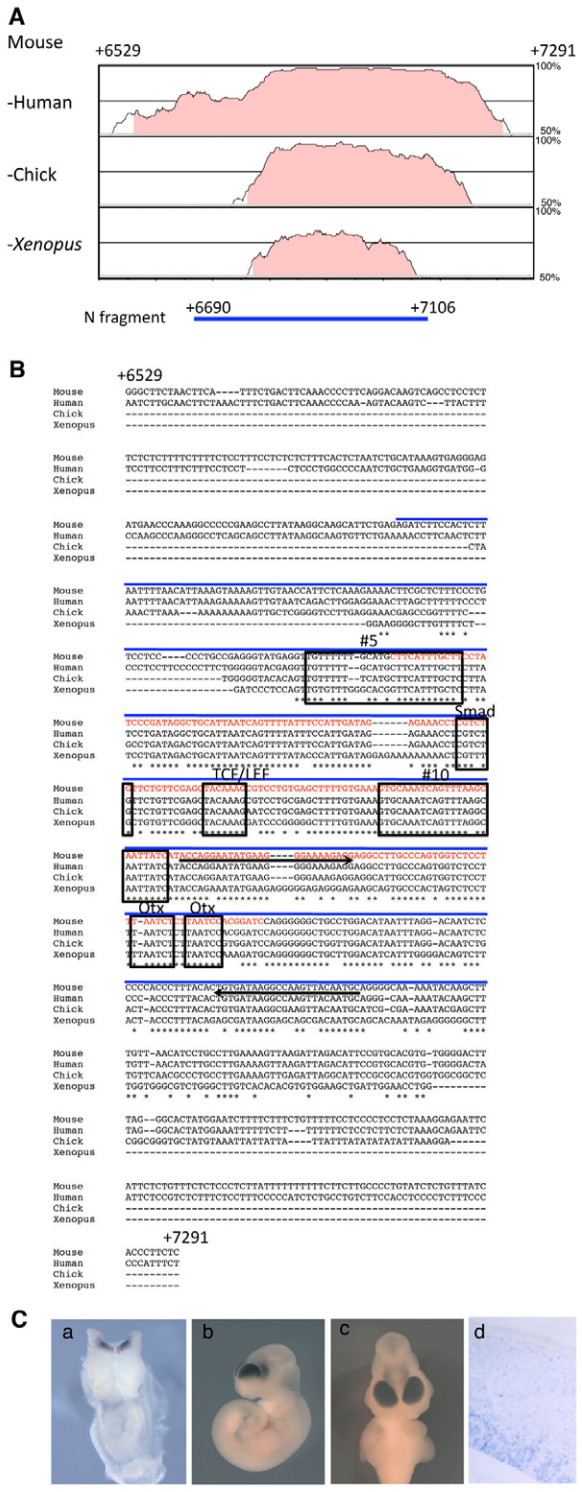

Fig. 4. Conservation of the *Emx2* θ domain among tetrapods. (**A**) Vista plot of each tetrapod *Emx2* θ domain against the mouse θ domain. (**B**) Nucleotide sequence of mouse, human, chick and *Xenopus* θ domains. A blue line indicates the *N* fragment. Smad, Tcf and Otx binding sites are boxed; #5 and #10 are sequences essential to the forebrain activity as demonstrated by the linker-scanner assay in Fig. 7. Arrowed lines indicate primers for ChIP analysis in Fig. 6C,D. (**Ca-d**) β-gal expression from the *lacZ* transgene directed by the *Xenopus* θ domain in mouse embryos at E8.5 (a) and E9.5 (b,c) and in the cortex at E15.5 (d). a,c, frontal views; b, lateral view with the anterior to the left; d, coronal section.

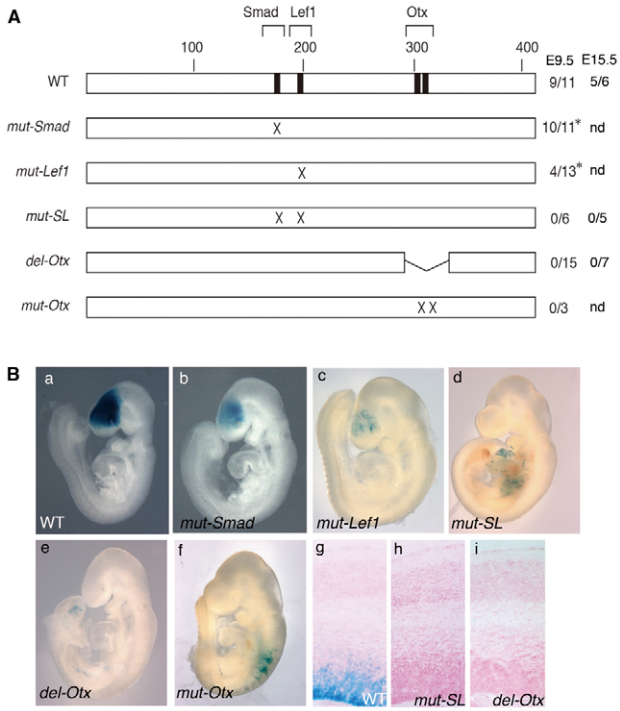

Fig. 5. Mutation analysis of the core sequences for the FB activity of the *N* fragment. (**A**) Schematic representation of the mutations made. The number of β-gal-positive embryos among total transgenic embryos generated is given at the right. Asterisks represents weak or faint expression as shown in Bb,c. (**Ba-i**) β-gal expression directed by the mutant *N* fragments indicated in E9.5 embryos (a-f) and in E15.5 cortex (g-i). (a-f) *2.1-Cre* transgenes conjugated with each mutant *N* fragment were injected into ROSA26R zygotes; (g-i) *2.1-lacZ* transgenes conjugated with each mutant N fragment were injected into wild-type zygotes.

different antibodies (Fig. 6C) and PCR primers were set up so that a 144 bp sequence, including the two Otx sites, was amplified (Fig. 4B). The ChIP assay with Otx2 antibodies indeed yielded the 144-bp products (Fig. 6C); they were confirmed by sequencing. The assay was also performed with E11.5 telencephalon. Otx2, Tcf4 and Tcf1 (Hnf1a – Mouse Genome Informatics) antibodies precipitated the enhancer (Fig. 6D), although we were unable to confirm Smad1/5/8 binding to the Smad site with the antibody used.

Linker scanner analysis of the *N* fragment

Otx, Tcf and Smad sites do not explain the deletion analysis of the *N* fragment into *R*, *S* and *T* subfragments or the requirement of the 5′ *R* subfragment (Fig. 3). It is also possible that sequences other than the Tcf, Smad and Otx sites are essential in the *N* fragment. A linker scanner assay was then conducted by replacing each 25 bp sequence of the *N* fragment with a 25 bp unrelated luciferase sequence (CTGGAGCCTGAGGAGTTCGCTGCCT); the sequence has no obvious consensus binding sites for known transcription factors by TRANSFAC database search. The mutant *N* fragments were numbered from #1, in which the first 25 bp was replaced with the luciferase sequence, to #17, in which the last 25 bp was replaced with the luciferase sequence. Mutant *N* fragments #1-4, #6, #7, #11, #12 and #14-17 exhibited almost the same activities as the wild-type *N* fragment (Fig. 7A). By contrast, #5,

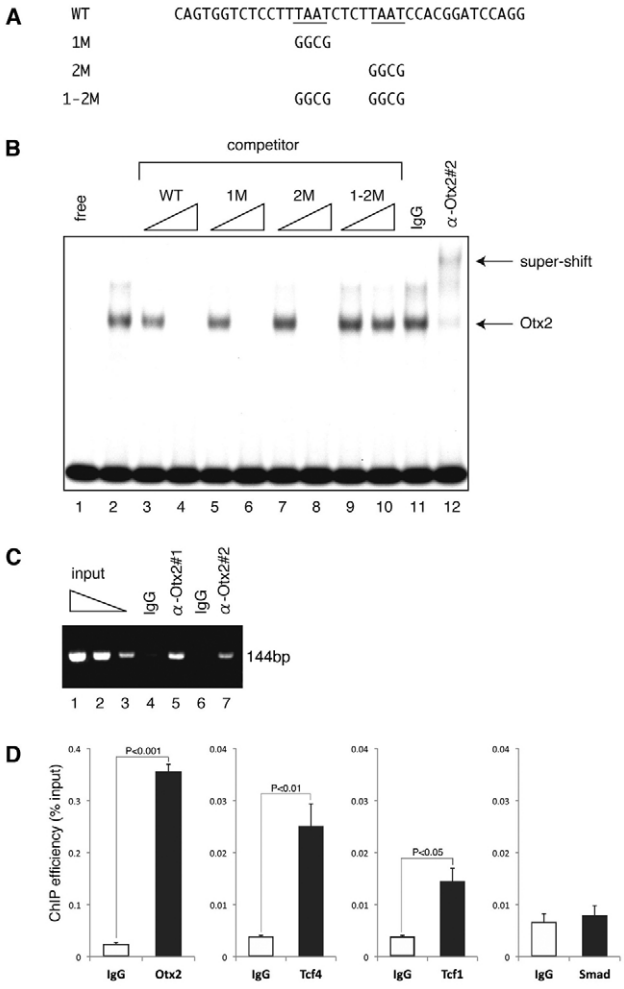

Fig. 6. Otx binding to Otx sites. (**A**) The nucleotide sequence of competitors. (**B**) Electrophoretic mobility shift assay for the Otx2 binding to Otx sites. The protein complex was lost in competition with a wild-type competitor (WT) and mutant competitors in which only one Otx site was mutated (1M or 2M), but not with the competitor in which two Otx sites were mutated (1-2M). The complex was super-shifted by anti-Otx2 antibody. (**C**) ChIP assay with neuralized P19 cells. Lanes 1, 2 and 3 give 10, 1 and 0.1% input amplification, respectively. Anti-Otx2 antibodies used (#1 and #2) are indicated in the Materials and methods. (**D**) ChIP assay with E11.5 telencephalon. Anti-Otx2, Tcf4, Tcf1 and Smad antibodies used are indicated in the Materials and methods. Data are expressed as mean ± s.d. and *P*-values are given in each panel.

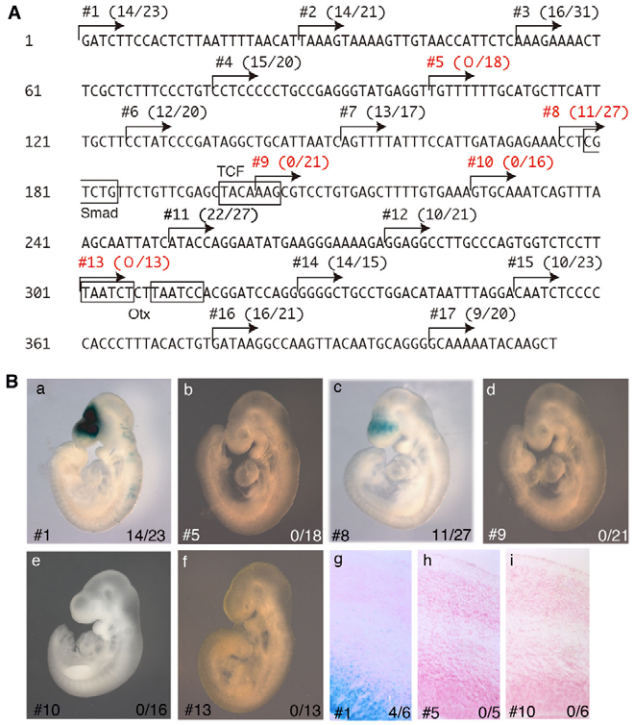

Fig. 7. Linker-scanner assay of the enhancer activity of the *N* fragment. (**A**) Each 25 bp block was replaced with a luciferase sequence. The *Cre* gene directed by each mutant *N* fragment was injected into ROSA26R zygotes and β-gal expression was examined at E9.5. The number of β-gal-positive embryos among total transgenic embryos generated with each mutant *N* fragment is provided in each block in parenthesis; mutations affecting the enhancer activity are indicated in red. With the #8 mutant *N* fragment, eleven transgenic embryos were β-gal-positive, but all of them exhibited weak β-gal expression, as shown in Bc. (**Ba-i**) Typical examples of β-gal expression in E9.5 embryos (a-f) and in E15.5 cortex (g-i) with the #1 (a,g), #5 (b,h), #8 (c), #9 (d), #10 (e,i) or #13 (f) mutant fragments. (a-f) *2.1-Cre* transgenes conjugated with each mutant *N* fragment were injected into ROSA26R zygotes; (g-i) *2.1-lacZ* transgenes conjugated with each mutant *N* fragment were injected into wild-type zygotes. The number of β-gal-positive embryos among transgenic embryos generated is indicated in each panel.

#9, #10 or #13 mutant *N* fragments exhibited no activity and the #8 mutant fragment exhibited only a weak activity in caudal telencephalon (Fig. 7A,Bb-f). The #8 sequence contains a Smad binding site, #9 a Tcf binding site and #13 two Otx binding sites. Of particular interest were the #5 and #10 sites that do not have a consensus sequence for the binding of known transcriptional factors; the #5 site explained the requirement of the *R* subfragment. Both were also essential to the activity in the E15.5 ventricular zone (Fig. 7Bg-i) and are well conserved among tetrapods (Fig. 4B). Despite intensive efforts, however, we have so far been unsuccessful in identifying the factors that bind to sequences #5 and #10.

FB enhancer mutant phenotype

To confirm the roles for the FB enhancer in *Emx2* expression, we next generated mouse mutants that lack this enhancer (Fig. 8A,B); the *G* domain (Fig. 3A) was first replaced with the *neo* cassette flanked by *loxP* sequences (FB-*neo* or *neo* allele) and the cassette was then deleted (ΔFB allele). Semi-quantitative RT-PCR and RNA in situ hybridization demonstrated that the *Emx2* expression in caudal forebrain primordium at E8.5 was lost in the homozygous FB enhancer mutants ($Emx2^{neo/neo}$ and $Emx2^{\Delta FB/\Delta FB}$ mutants; Fig. 8Bc,Ca,e). However, at E9.5 and E10.5, *Emx2* expression decreased to about half, but was present in both $Emx2^{neo/neo}$ and $Emx2^{\Delta FB/\Delta FB}$ mutants (Fig. 8Bc,Cb-d,f-h). The loss of the *Emx2* expression in caudal forebrain primordium at E8.5 and the reduction in E10.5 telencephalon was further confirmed by quantitative RT-PCR (Fig. 8D). The level of *Emx2* expression in E8.5 mutant head and in E10.5 diencephalon was less than 10% of that in wild-type counterparts, whereas the level of *Emx2* expression in E10.5 mutant telencephalon was about 40% of that in wild-type telencephalon. Sequencing of the

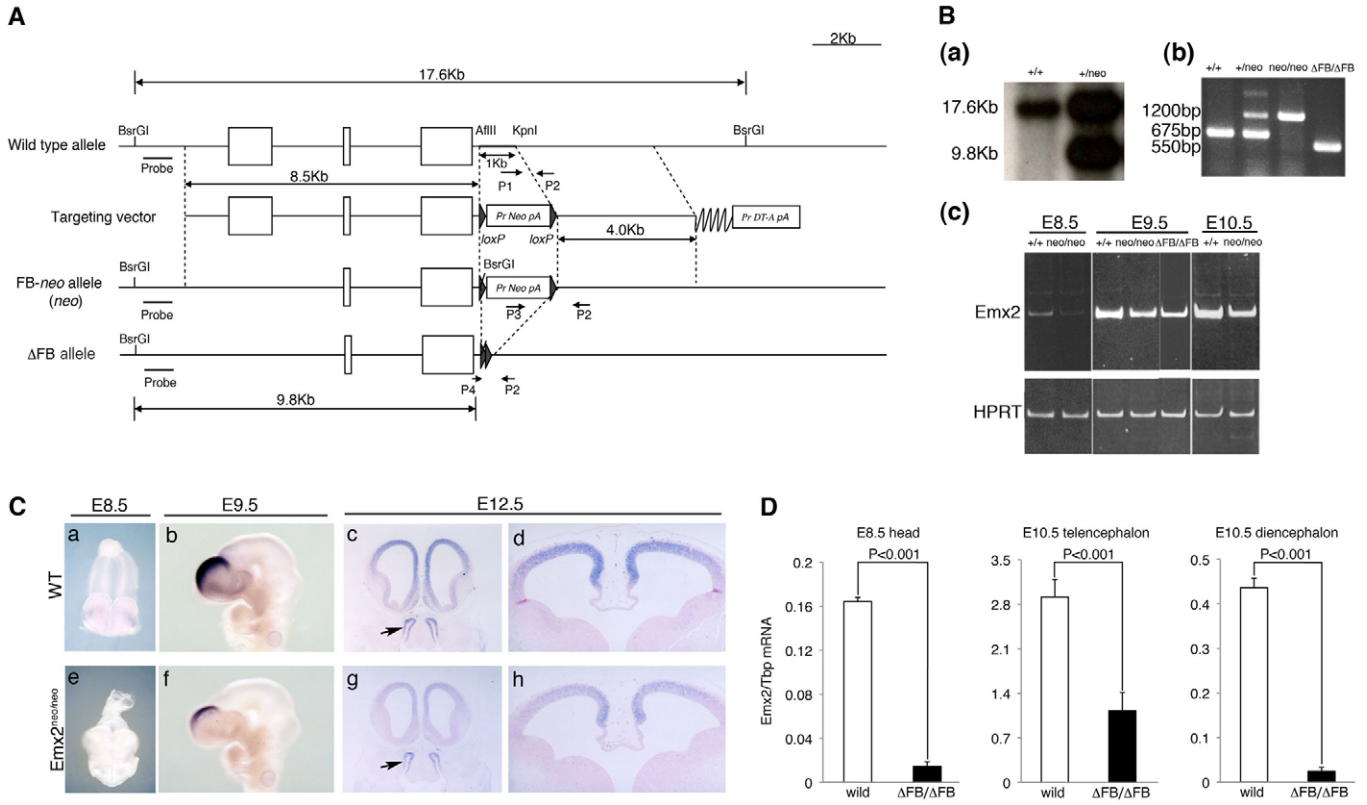

Fig. 8. Targeted disruption of the forebrain enhancer. (**A**) Schematic representation of a wild-type allele, targeting vector, FB-*neo* allele and ΔFB allele. White boxes represent *Emx2* exons. The 1 kb *AflII*/*KpnI* fragment covering the θ domain was replaced with a neomycin resistance gene with a *Pgk1* promoter and SV40 polyadenylation signal (*PrNeopA*) flanked by *loxP* sequences (black triangles; FB/*neo* or *neo* allele); ΔFB allele was obtained by *Cre*-mediated *loxP* recombination. Zigzag line indicates the vector-derived sequences and *PrDT-ApA* is a diphtheria toxin A fragment gene with an *MC1* promoter and rabbit β-globin gene poly A signal for the negative selection (Yagi et al., 1990). Lengths of the homologous regions in the targeting vector were 8.5 and 4.0 kb at the 5′ and 3′ ends, respectively. Locations of the probe for the Southern blotting in Ba and p1-p4 primers for routine genotyping shown in Bb are indicated. (**Ba-c**) Characterization of the FB/*neo* and ΔFB allele. (a) An example of Southern blotting for homologous recombinant ES cells digested by BsrGI with the probe indicated in A; (b) an example of routine genotyping by PCR with p1-p4 primers; (c) semi-quantitative RT-PCR for the *Emx2* expression in wild-type, $Emx2^{neo/neo}$ and $Emx2^{\Delta FB/\Delta FB}$ mutant brains at E8.5, E9.5 and E10.5. (**Ca-h**) RNA in situ hybridization of the *Emx2* expression in wild-type and $Emx2^{neo/neo}$ embryos at E8.5, E9.5 and E12.5. a,e, frontal views; b,f, lateral views with anterior to the left; c,d,g,h, coronal sections at anterior (c,g) and posterior (d,h) telencephalon. The expression in the nasal epithelium (arrows) was unchanged in the mutants. (**D**) Quantitative RT-PCR for the *Emx2* transcripts in E8.5 rostral head and in E10.5 telencephalon and diencephalon. Data are expressed as mean ± s.d. and *P*-values are given in each panel.

amplified products with E10.5 mutant telencephalon indicated that the products are indeed *Emx2* transcripts. Therefore, we conclude that the FB enhancer is responsible for *Emx2* expression in caudal forebrain primordium at E8.5, but another enhancer must exist for *Emx2* expression in telencephalon.

Emx2 function in the development of caudal forebrain primordium is represented in the defects of *Emx2* and *Otx2* double mutants ($Emx2^{-/-};Otx2^{+/-}$), in which the thalamic eminence, ventral thalamus (prethalamus), dorsal thalamus (thalamus) and non-commissure regions of the pretectum are lost (Fig. 9Aa,b) (Suda et al., 2001; Kimura et al., 2005). $Emx2^{neo/neo};Otx2^{+/-}$ and $Emx2^{\Delta FB/\Delta FB};Otx2^{+/-}$ mutants lost these diencephalic structures as did $Emx2^{-/-};Otx2^{+/-}$ (Fig. 9Ac,d). This is consistent with the loss of *Emx2* expression in the E8.5 $Emx2^{neo/neo}$ and $Emx2^{\Delta FB/\Delta FB}$ mutants, confirming that the FB enhancer is solely responsible for *Emx2* expression in E8.5 caudal forebrain primordium.

Emx2 function in early telencephalon or medial pallium development is represented in $Emx1^{-/-};Emx2^{-/-}$ double mutants (Shinozaki et al., 2004); the loss of medial pallium is significant in $Emx2^{-/-}$ mutants and remarkable in $Emx1^{-/-};Emx2^{-/-}$ mutants (Fig. 9Ba-c). The loss was moderate in $Emx2^{\Delta FB/\Delta FB}$, $Emx1^{-/-};Emx2^{neo/neo}$ and $Emx1^{-/-};Emx2^{\Delta FB/\Delta FB}$ mutants (Fig. 9Bd-f). The cortical hem, where the FB enhancer is inactive, develops into fimbria. At E18.5, histologically dentate gyrus is lost in $Emx2^{-/-}$ mutants, and fimbria, dentate gyrus and hippocampus are lost in $Emx1^{-/-};Emx2^{-/-}$ mutants (Fig. 9Ca-c) (Shinozaki et al., 2004). Dentate gyrus was lost, but fimbria developed, and hippocampus was moderately reduced in $Emx1^{-/-};Emx2^{neo/neo}$ and $Emx1^{-/-};Emx2^{\Delta FB/\Delta FB}$ mutants (Fig. 9Cd-f).

Subsequent *Emx2* functions in Cajal-Retzius cell development and cortical lamination are also demonstrated in *Emx1;Emx2* double mutant cortex (Fig. 9Da-f) (Shinozaki et al., 2002). Histologically, defects in cortical laminar structure were moderate in the $Emx1^{-/-};Emx2^{neo/neo}$ and $Emx1^{-/-};Emx2^{\Delta FB/\Delta FB}$ mutant cortex (Fig. 9Dg-l) when compared with the $Emx1^{-/-};Emx2^{-/-}$ defect. The cortical hem is the major source of Cajal-Retzius cells. Reelin-positive cells are lost in $Emx1^{-/-};Emx2^{+/-}$ mutant cortex (Fig. 9Dc,f) (Shinozaki et al., 2002), but were present in $Emx1^{-/-};Emx2^{neo/neo}$ and $Emx1^{-/-};Emx2^{\Delta FB/\Delta FB}$ mutants (Fig. 9Di,l). Furthermore, interneurons are scarce in $Emx1^{-/-};Emx2^{+/-}$ mutant cortex owing to the failure of their tangential migration, causing

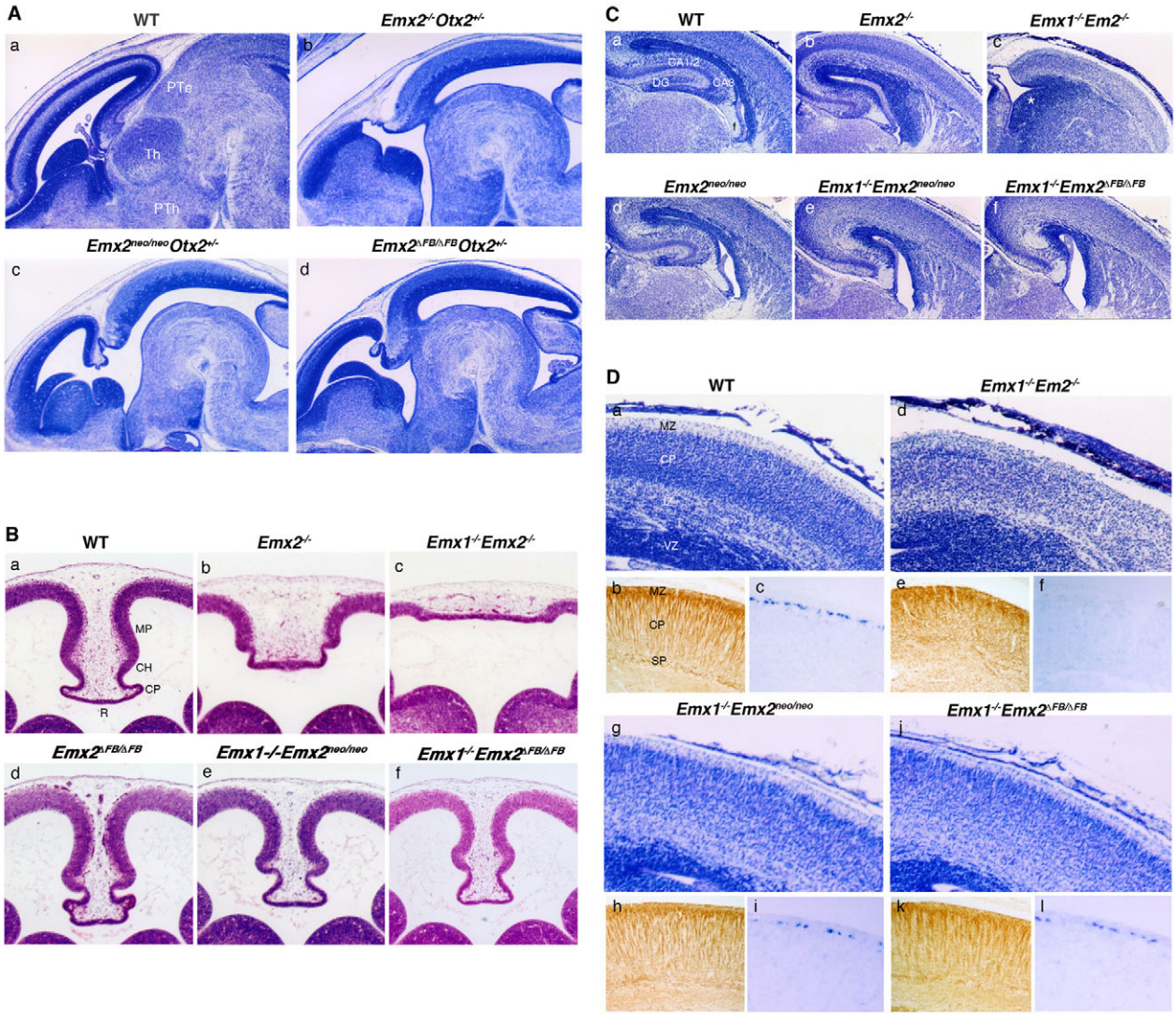

Fig. 9. Mutant phenotypes. (**Aa-d**) Loss of diencephalon in E15.5 *Emx2;Otx2* double mutants indicated, stained with Cresyl Violet. PTe, pretectum; PTh, prethalamus; Th, thalamus. (**Ba-f**) Medial pallium development in E12.5 *Emx1;Emx2* double mutants indicated, stained with Hematoxylin and Eosin. CH, cortical hem; CP, choroid plexus; MP, medial pallium; R, choroidal roof. (**Ca-f**) Medial pallium development in E18.5 *Emx1;Emx2* double mutants indicated, stained with Cresyl Violet. The asterisk indicates the hyperplastic ganglionic eminences in $Emx1^{-/-};Emx2^{-/-}$ mutants. CA1/2 and CA3, each field of hippocampus; DG, dentate gyrus; f, fimbria. (**Da-l**) Cortical layer formation in E18.5 *Emx1;Emx2* double mutants indicated. a,d,g,j, stained with Cresyl Violet; b,e,h,k, immunostained with anti-MAP1 antibody; c,f,i,l, RNA in situ hybridization of reelin expression for Cajal-Retzius cells in the marginal zone. CP, cortical plate; IZ, intermediate zone; MZ, Marginal zone; SP, subplate; VZ, ventricular zone.

the hyperplasia of ganglionic eminences (Fig. 9Ca,c) (Shinozaki et al., 2002). However, ganglionic eminences were apparently normal in $Emx1^{-/-};Emx2^{neo/neo}$ and $Emx1^{-/-};Emx2^{\Delta FB/\Delta FB}$ mutants (Fig. 9Ce,f). Therefore, the telencephalic phenotypes of the double mutants with $Emx1^{-/-}$ indicated the hypomorphic nature of $Emx2^{neo/neo}$ and $Emx2^{\Delta FB/\Delta FB}$ mutations and the presence of the second enhancer for *Emx2* expression in telencephalon. No difference was apparent in any of these double mutant phenotypes between $Emx2^{neo/neo}$ and $Emx2^{\Delta FB/\Delta FB}$ mutants.

Enhancer activities of the *Xenopus* θ domain

The θ domain is conserved in the *Xenopus Emx2* locus. Otx, Tcf and Smad binding sites are perfectly conserved, the #10 site has only one base change among its 25 bases, and 20 bases out of the 25 are the same in the #5 site (Fig. 4B). The enhancer activity of the *Xenopus* θ domain was then examined in mouse forebrain. It indeed exhibited activities in caudal forebrain primordium at E8.5, in dorsal telencephalon at E9.5 and in the ventricular, but not marginal, zone at E15.5 (Fig. 4C). These activities of the *Xenopus* θ domain were almost the same as those of the mouse; however, the shift of its activity from diencephalon to telencephalon took place at E9.5. Thus, the FB enhancer is most probably responsible for the basal *Emx2* functions in tetrapod forebrain, but not for the functions unique to mammals; the FB enhancer lacked the activities in the cortical hem and Cajal-Retzius cells and its activity was not graded in the cortex.

DISCUSSION

We expected that different enhancers direct each *Emx2* expression: in caudal forebrain primordium at the 3- to 6-somite stage, in dorsal telencephalon during its initial development and in the cortical

ventricular zone and Cajal-Retzius cells during cortical lamination (Kurokawa et al., 2004a; Kurokawa et al., 2004b). Unexpectedly, however, the FB enhancer identified in this study had activities in caudal forebrain primordium, in dorsal telencephalon and in the ventricular zone. Not only Tcf and Smad sites, but also Otx sites and two other sites for unknown factors – sequences #5 (TGTTTTTTGCATGCTTCATTTGCTT) and #10 (GTGCAA-ATCAGTTTAAGCAATTATC) – were essential to all these activities. The FB enhancer mutants indicated that the enhancer is solely responsible for the *Emx2* expression in caudal forebrain primordium but that there is another enhancer for the *Emx2* expression unique to mammalian telencephalon.

The FB enhancer is conserved among tetrapod *Emx2* loci; the *Xenopus* θ domain exhibited enhancer activities in mouse caudal forebrain primordium at E8.5, in dorsal telencephalon at E9.5 and in the ventricular zone at E15.5. These activities of the *Xenopus* θ domain are almost the same as those of the mouse. Moreover, Otx, Tcf, Smad, #5 and #10 sites are well conserved among tetrapod θ domains, suggesting that the upstream mechanisms that control the θ domain enhancer activity at each site must also be conserved among tetrapods. The θ domain enhancer and its upstream factors thus would have been established in ancestor tetrapods to shoulder the *Emx2* functions in forebrain development common to tetrapod *Emx2* genes.

The change in the active sites of the (ζ–η–θ) domain solved a question about early *Emx2* expression. Previous cell lineage analysis with *Cre* knock-in into the mouse *Emx2* locus indicated that although most of diencephalic cells do not express *Emx2* at E9.5, they are descendants of *Emx2*-positive caudal forebrain primordium at E8.5 (Kimura et al., 2005). They precisely coincide with the cells in which the (ζ–η–θ) domain is active at E9.5 (Fig. 2J). The cell lineage analysis, however, could not tell whether *Emx2*-positive telencephalic cells at E9.5 are descendants of *Emx2*-positive caudal forebrain primordium at E8.5 or if the *Emx2* expression newly begins in the telencephalic cells that have not expressed *Emx2* at E8.5. The activity shift of the (ζ–η–θ) domain apparently suggested that the FB enhancer initially does not have an activity in telencephalic primordium when it is active in diencephalic precursor cells. The profile of the (ζ–η–θ) domain activities thus suggests that the endogenous *Emx2* expression first takes place in diencephalic precursor cells at the 3- to 4-somite stage but becomes suppressed by E9.5 in their descendant cells. Coincidentally, the endogenous *Emx2* expression takes place in dorsal telencephalon by E9.5. In *Xenopus* at early neurula, it was reported that *Emx2* expression is first found in an area that generates diencephalon, being distinct from *Emx1*-positive future telencephalon; soon after neural tube closure, *Emx2* is transcribed in almost the same domain as *Emx1* at the level of the dorsal telencephalon (Pannese et al., 1998). This is also likely to be the case in chick forebrain development (Bell et al., 2001).

This study opens the question how the temporal changes in the forebrain activities are regulated. Otx is essential but cannot explain the forebrain activity specific to the caudal forebrain primordium at E8.5; at this stage, Otx2 is expressed in the entire anterior neuroectoderm and Otx1 expression also starts in the ectoderm (Simeone et al., 1992). Wnt and Bmp proteins are expressed in anterior neuroectoderm and/or surface ectoderm adjacent to the neuroectoderm; they are essential to but cannot explain the *Emx2* expression specific to the caudal forebrain primordium. After closure of the neural tube, Wnt and Bmp proteins continue to be expressed at the dorsal midline of diencephalon. Otx2 and Otx1 also continue to be expressed in diencephalon. Thus these cannot explain why the FB enhancer activity ceases in diencephalon later than E9.5. When the neural plate is closed at the telencephalic level, Bmp proteins are expressed in the choroidal roof, choroid plexus and cortical hem (Furuta et al., 1997). A series of Wnt proteins are also expressed in medial pallium in a nested pattern (Grove et al., 1998; Lee et al., 2000). Otx2 is also expressed in these sites (Kurokawa et al., 2004a; Kurokawa et al., 2004b). The forebrain activity appears to take place from the caudodorsomedial telencephalon (Fig. 2H,I; Fig. 3Cc,d), and Wnt, Bmp and Otx would explain the forebrain activity in telencephalon. However, it is a question why the FB enhancer, which is regulated by Otx, Tcf and Smad, does not have activity in the cortical hem, choroid plexus or roof.

At subsequent stages Wnt, Bmp and Otx2 expression persists in the dorsomedial telencephalon; after E9.5, Otx2 expression is lost in neopallium, ganglionic eminences and the hypothalamus (Simeone et al., 1992; Kurokawa et al., 2004b), but Otx1 expression continues to be expressed in the entire cortex, including the cortical hem. At E15.5, Otx2 is not expressed in the ventricular zone of the neopallium, whereas Otx1 is expressed in the entire cortical ventricular zone (Simeone et al., 1993; Frantz et al., 1994). Otx1 would thus explain the forebrain activity in the ventricular zone, but *Emx2* is expressed in the ventricular zone of *Otx1* mutants (Suda et al., 1997) (our unpublished data). The Tcf and Smad sites in the FB enhancer were essential to its activity even in the lateral and ventral pallium; however, the source of signalings for Tcf and Smad expression in the pallium is not clear. Identification of the factors that bind to #5 and #10 sites is the first step to address these questions.

The FB enhancer mutants indicated the presence of the second enhancer for the *Emx2* expression in telencephalon. In $Emx2^{\Delta FB/\Delta FB}$ mutant telencephalon at E9.5 and E10.5, *Emx2* expression was reduced but present at about 40% strength; $Emx1^{-/-};Emx2^{\Delta FB/\Delta FB}$ mutant phenotypes in medial pallium development and cortical lamination were much milder than $Emx1^{-/-};Emx2^{-/-}$ phenotypes. In contrast to the FB enhancer, the second enhancer must be responsible for the graded *Emx2* expression, exhibiting activity in the cortical hem and Cajal-Retzius cells. Hippocampal structures have remarkably evolved in amniotes (Butler and Hodos, 2005) and the cortical hem is thought to be the organizing center of the medial pallium development (Mangale et al., 2008). Graded *Emx2* expression in the cortex, together with *Pax6* expression in the reciprocal gradient, has been suggested to regulate area patterning in mammalian telencephalon (O'Leary and Nakagawa, 2002). Laminar structure and area patterning are characteristic to mammalian telencephalon. The second enhancer must thus be unique to mammals, and its identification, together with the determination of its upstream factors, will bring us valuable information on the evolution of mammalian telencephalon.

Acknowledgements

We are indebted to the Laboratory for Animal Resources and Genetic Engineering of RIKEN CDB for animal housing and mutant mouse production. This work was supported by a Grant-in-Aid for Creative Scientific Research from the Japan Society for the Promotion of Science.

Competing interests statement

The authors declare no competing financial interests.

References

Agata, Y., Katakai, T., Ye, S. K., Sugai, M., Gonda, H., Honjo, T., Ikuta, K. and Shimizu, A. (2001). Histone acetylation determines the developmentally regulated accessibility for T cell receptor gamma gene recombination. *J. Exp. Med.* **193**, 873-880.

Bell, E., Ensini, M., Gulisano, M. and Lumsden, A. (2001). Dynamic domains of gene expression in the early avian forebrain. *Dev. Biol.* **236**, 76-88.
Butler, A. B. and Hodos, W. (2005). Limbic telencephalon. In *Comparative Vertebrate Neuroanatomy: Evolution and Adaptation,* 2nd edn (ed. A. B. Butler and W. Hodos), pp. 611-634. John Wiley and Sons.
Couronne, O., Poliakov, A., Bray, N., Ishkhanov, T., Ryaboy, D., Rubin, E., Pachter, L. and Dubchak, I. (2003). Strategies and tools for whole-genome alignments. *Genome Res.* **13**, 73-80.
Dignam, J. D., Lebovitz, R. M. and Roeder, R. G. (1983). Accurate transcription initiation by RNA polymerase II in a soluble extract from isolated mammalian nuclei. *Nucleic Acids Res.* **11**, 1475-1489.
Frantz, G. D., Weimann, J. M., Levin, M. E. and McConnell, S. K. (1994). Otx1 and Otx2 define layers and regions in developing cerebral cortex and cerebellum. *J. Neurosci.* **14**, 5725-5740.
Fruta, Y., Piston, D. W. and Hogan, B. L. M. (1997). Bone morphogenetic proteins (BMPs) as regulators of dorsal forebrain development. *Development* **124**, 2203-2212.
Grove, E. A., Tole, S., Limon, J., Yip, Y. and Ragsdale, C. W. (1998). The hem of the embryonic cerebral cortex is defined by the expression of multiple *Wnt* genes and is compromised in *Gli3*-deficient mice. *Development* **125**, 2315-2325.
Gulisano, M., Broccoli, V., Pardini, C. and Boncinelli, E. (1996). *Emx1* and *Emx2* show different patterns of expression during proliferation and differentiation of the developing cerebral cortex in the mouse. *Eur. J. Neurosci.* **8**, 1037-1050.
Heinemeyer, T., Wingender, E., Reuter, I., Hermjakob, H., Kel, A. E., Kel, O. V., Ignatieva, E. V., Ananko, E. A., Podkolodnaya, O. A., Kolpakov, F. A. et al. (1998). Databases on transcriptional regulation: TRANSFAC, TRRD and COMPEL. *Nucleic Acids Res.* **26**, 362-367.
Kimura, C., Shen, M. M., Takeda, N., Aizawa, S. and Matsuo, I. (2001). Complementary functions of Otx2 and Cripto in initial patterning of mouse epiblast. *Dev. Biol.* **235**, 12-32.
Kimura, J., Suda, Y., Kurokawa, D., Hossain, Z. M., Nakamura, M., Takahashi, M., Hara, A. and Aizawa, S. (2005). Emx2 and Pax6 function in cooperation with Otx2 and Otx1 to develop caudal forebrain primordium that includes future archipallium. *J. Neurosci.* **25**, 5097-5108.
Kucharczuk, K. L., Love, C. M., Dougherty, N. M. and Goldhamer, D. J. (1999). Fine-scale transgenic mapping of the MyoD core enhancer: MyoD is regulated by distinct but overlapping mechanisms in myotomal and non-myotomal muscle lineages. *Development* **126**, 1957-1965.
Kurokawa, D., Kiyonari, H., Nakayama, R., Kimura-Yoshida, C., Matsuo, I. and Aizawa, S. (2004a). Regulation of Otx2 expression and its functions in mouse forebrain and midbrain. *Development* **131**, 3319-3331.
Kurokawa, D., Takasaki, N., Kiyonari, H., Nakayama, R., Kimura-Yoshida, C., Matsuo, I. and Aizawa, S. (2004b). Regulation of Otx2 expression and its functions in mouse epiblast and anterior neuroectoderm. *Development* **131**, 3307-3317.
Lee, S. M. K., Tole, S., Grove, E. and McMahon, A. P. (2000). A local Wnt-3a signal is required for development of the mammalian hippocampus. *Development* **127**, 457-467.
Mallamaci, A., Iannone, R., Briata, P., Pintonello, L., Mercurio, S., Boncinelli, E. and Corte, G. (1998). EMX2 protein in the developing mouse brain and olfactory area. *Mech. Dev.* **77**, 165-172.
Mangale, V. S., Hirokawa, K. E., Satyaki, P. R. V., Gokulchandran, N., Chikbire, S., Subramanian, L., Shetty, A. S., Martynoga, B., Paul, J., Mai, M. V. et al. (2008). Lhx2 selector activity specifies cortical identity and suppresses hippocampal organizer fate. *Science* **319**, 304-309.
Matsuo, I., Kuratani, S., Kimura, C., Takeda, N. and Aizawa, S. (1995). Mouse Otx2 functions in the formation and patterning of rostral head. *Genes Dev.* **9**, 2646-2658.
Mayor, C., Brudno, M., Schwartz, J. R., Poliakov, A., Rubin, E. M., Frazer, K. A., Pachter, L. S. and Dubchak, I. (2000). VISTA: visualizing global DNA sequence alignments of arbitrary length. *Bioinformatics* **16**, 1046-1047.
Miyamoto, N., Yoshida, M., Kuratani, S., Matsuo, I. and Aizawa, S. (1997). Defects of urogenital development in mice lacking Emx2. *Development* **124**, 1653-1664.
O'Leary, D. D. M. and Nakagawa, Y. (2002). Patterning centers, regulatory genes and extrinsic mechanisms controlling arealization of the neocortex. *Curr. Opin. Neurobiol.* **12**, 14-25.
Pacherník, J., Bryja, V., Esner, M., Kubala, L., Dvorák, P. and Hampl, A. (2005). Neural differentiation of pluripotent mouse embryonal carcinoma cells by retinoic acid: inhibitory effect of serum. *Physiol. Res.* **54**, 115-122.
Pannese, M., Lupo, G., Kablar, B., Boncinelli, E., Barsacchi, G. and Vignali, R. (1998). The *Xenopus* Emx genes identify presumptive dorsal telencephalon and are induced by head organizer signals. *Mech. Dev.* **73**, 73-83.
Pellegrini, M., Mansouri, A., Simeone, A., Boncinelli, E. and Gruss, P. (1996). Dentate gyrus formation requires *Emx2*. *Development* **122**, 3893-3898.
Shibata, M., Kurokawa, D., Nakao, H., Ohmura, T. and Aizawa, S. (2008). MicroRNA-9 modulates Cajal-Retzius cell differentiation by suppressing Foxg1 expression in mouse medial pallium. *J. Neurosci.* **28**, 10415-10421.
Shinozaki, K., Miyagi, T., Yoshida, M., Miyata, T., Ogawa, M., Aizawa, S. and Suda, Y. (2002). Absence of Cajal-Retzius cells and subplate neurons associated with defects of tangential cell migration from ganglionic eminence in *Emx1/2* double mutant cerebral cortex. *Development* **129**, 3479-3492.
Shinozaki, K., Yoshida, M., Nakamura, M., Aizawa, S. and Suda, Y. (2004). Emx1 and Emx2 cooperate in initial phase of archipallium development. *Mech. Dev.* **121**, 475-489.
Simeone, A., Acampora, D., Gulisano, M., Stornaiuolo, A. and Boncinelli, E. (1992). Nested expression domains of four homeobox genes in developing rostral brain. *Nature* **358**, 687-690.
Simeone, A., Acampora, D., Mallamaci, A., Stornaiuolo, A., D'Apice, M. R., Nigro, V. and Boncinelli, E. (1993). A vertebrate gene related to orthodenticle contains a homeodomain of the bicoid class and demarcates anterior neuroectoderm in the gastrulating mouse embryo. *EMBO J.* **12**, 2735-2747.
Suda, Y., Matsuo, I. and Aizawa, S. (1997). Cooperation between *Otx1* and *Otx2* genes in developmental patterning of rostral brain. *Mech. Dev.* **69**, 125-141.
Suda, Y., Hossain, Z. M., Kobayashi, C., Hatano, O., Yoshida, M., Matsuo, I. and Aizawa, S. (2001). Emx2 directs the development of diencephalon in cooperation with Otx2. *Development* **128**, 2433-2450.
Svingen, T., Spiller, C. M., Kashimada, K., Harley, V. R. and Koopman, P. (2009). Identification of suitable normalizing genes for quantitative real-time RT-PCR analysis of gene expression in fetal mouse gonads. *Sex. Dev.* **3**, 194-204.
Takasaki, N., Kurokawa, D., Nakayama, R., Nakayama, J. and Aizawa, S. (2007). Acetylated YY1 regulates Otx2 expression in anterior neuroectoderm at two cis-sites 90 kb apart. *EMBO J.* **26**, 1649-1659.
Takiguchi-Hayashi, K., Sekiguchi, M., Ashigaki, S., Takamatsu, M., Hasegawa, H., Suzuki-Migishima, R., Yokoyama, M., Nakanishi, S. and Tanabe, Y. (2004). Generation of reelin-positive marginal zone cells from the caudomedial wall of telencephalic vesicles. *J. Neurosci.* **24**, 2286-2295.
Theil, T., Aydin, S., Koch, S., Grotewold, L. and Ruther, U. (2002). Wnt and Bmp signalling cooperatively regulate graded Emx2 expression in the dorsal telencephalon. *Development* **129**, 3045-3054.
Visel, A., Blow, M. J., Li, Z., Zhang, T., Akiyama, J. A., Holt, A., Plajzer-Frick, I., Shoukry, M., Wright, C., Chen, F. et al. (2009). ChIP-seq accurately predicts tissue-specific activity of enhancers. *Nature* **457**, 854-858.
Yagi, T., Ikawa, Y., Yoshida, K., Shigetani, Y., Takeda, N., Mabuchi, I., Yamamoto, T. and Aizawa, S. (1990). Homologous recombination at c-fyn locus of mouse embryonic stem cells with use of diphtheria toxin A-fragment gene in negative selection. *Proc. Natl. Acad. Sci. USA* **87**, 9918-9922.
Yoshida, M., Suda, Y., Matsuo, I., Miyamoto, N., Takeda, N., Kuratani, S. and Aizawa, S. (1997). Emx1 and Emx2 functions in development of dorsal telencephal telencephalon. *Development* **124**, 101-111.
Yoshida, M., Assimacopoulos, S., Jones, K. R. and Grove, E. A. (2006). Massive loss of Cajal-Retzius cells does not disrupt neocortical layer order. *Development* **133**, 537-545.